



Dosimetric verification of clinical radiotherapy treatment planning system

Dozimetrijska verifikacija kliničkog sistema za planiranje radioterapije

Goran Kolarević*†, Dražan Jaroš*†, Goran Marošević*†, Dejan Ignjatić*,
Dragoljub Mirjanić†

*International Medical Centers Affidea, Center for Radiation Therapy, Banja Luka,
Bosnia and Herzegovina; †University of Banja Luka, Faculty of Medicine, Bosnia and
Herzegovina

Abstract

Background/Aim. In the past two decades, we have witnessed the emergence of new radiation therapy techniques, radiotherapy treatment planning system (TPS) with calculating algorithms for the dosage calculation in a patient, units for multislice computed tomography (CT) and image-guided treatment delivery. The aim of the study was investigating the significant difference in dosimetric calculation of radiotherapy TPS in relation to the values obtained by measuring on the linear accelerator (LINAC), and the accuracy of dosimetric calculation between calculating algorithms Analytical Anisotropic Algorithm (AAA) and Acuros XB in various tissues and photon beam energies. **Methods.** For End-to-End test we used the heterogeneous phantom CIRS Thorax002LFC, which anatomically represents human torso with a set of inserts known as relative electron densities (RED) for obtaining a CT calibration curve, comparable to the “reference” CIRS 062M phantom. For the AAA and Acuros XB algorithms and for 6 MV and 16 MV photon beams in the TPS Varian Eclipse 13.6, four 3D conformal (3DCRT), and one intensity modulated (IMRT) and volumetric modulated arc

(VMAT) radiotherapy plans were made. Measurements of the absolute dose in Thorax phantom, by PTW-Semiflex ionization chamber, were carried out on three Varian-DHX LINACs. **Results.** The difference between “reference” and measured CT conversion curves in the bone area was 3%. For 476 phantom measurements, the difference between measured and TPS calculated dose of 3–6%, was found in 30 (6.3%) cases. According to regression analysis, the standardized Beta coefficient for relative errors, 6 MV vs. 16 MV, was 0.337 (33.7%, $p < 0.001$). Mean relative errors for AAA and Acuros XB, using Mann-Whitney test, for bones were 1.56% and 2.64%, respectively ($p = 0.004$). **Conclusion.** End-to-End test on Thorax002LFC phantom proved the accuracy of TPS dose calculation in relation to the one delivered to a patient by LINAC. There was a significant difference for photon energies relative errors (higher values are obtained for 16 MV vs. 6 MV). A statistically significant minor relative error in AAA vs. Acuros XB was found for the bone.

Key words:
algorithms; models, theoretical; radiotherapy;
radiotherapy planning, computer-assisted; thorax.

Apstrakt

Uvod/Cilj. Poslednje dve decenije svedoci smo pojave novih tehnika radijacione terapije, sistema za planiranje tretmana (SPT) radioterapijom sa algoritimima za izračunavanje doze kod bolesnika, jedinica za višerednu (*multislice*) kompjuterizovanu tomografiju (KT) i slikomvođeno praćenje. Cilj rada je bio da se utvrdi da li postoji značajna razlika u izračunavanju doze primenom SPT u odnosu na vrednosti dobijene merenjem na linearnom akceleratoru (LINAC), kao i razlika u tačnosti dozimetrijskog proračuna kalkulacionih algoritama *Analytical Anisotropic Algorithm (AAA)* i *Acuros XB* u zavisnosti od tipa tkiva i energije fotonskih snopova. **Metode.** Za *End-to-End* test koristili smo heterogeni fantom CIRS Thor-

ax002LFC, koji anatomski odgovara ljudskom torzu sa setom umetaka poznate relativne elektronske gustine za dobijanje KT kalibracione krive, koja se poredi sa referentnim vrednostima, dobijenim CIRS 062M fantomom. Za *AAA* i *Acuros XB* algoritme kao i za 6 MV i 16 MV fotonske snopove u *SPT Varian Eclipse 13,6*, napravljena su četiri 3D konformalna (3DCRT), jedan intenzitetom modulisan (IMRT) i jedan zapreminski modulisan lučni (VMAT) plan radioterapije. Merenja apsolutne doze u mernim pozicijama *Thorax* fantoma, jonizacionom komorom *PTW-Semiflex*, sprovedena su na tri *Varian-DHX* LINAC-a. **Rezultati.** Razlika „referentne” i merene KT konverziona krive u oblasti kostiju bila je 3%. Od ukupno 476 mernih tačaka, razlika između izmerene i SPT izračunate doze od 3–6%, je nađena u 30 tačaka (6.3%).

Regresionom analizom je utvrđen standardizovani koeficijent Beta za relativne greške, 6 MV vs. 16 MV, koji je iznosio 0,337 (33,7%, $p < 0,001$). Srednje vrednosti relativnih grešaka za AAA i Acuros XB za kosti, koristeći Mann-Whitney test, su bile 1,56% i 2,64% ($p = 0,004$). **Zaključak.** End-to-End test na Thorax002LFC fantomu je dao potvrdu ispravnog računanja doze primenom SPT u odnosu na dozu isporučenu pacijentu pomoću LINAC-a.

Introduction

It is beyond any doubt that modern radiotherapy (RT) technologically represents the most complex branch of medicine today. In the treatment of malignant diseases, as a cure, we use ionizing radiation directed towards the volume in which the tumor cells are located in order to permanently destroy them with the maximum possible protection of the surrounding healthy tissue.

In the past two decades, with the development of information technology, we have witnessed the emergence of the new ones: radiation therapy techniques, radiotherapy treatment planning systems (TPS) with calculating algorithms for the dosage calculation in a patient, units for multislice computed tomography (CT) and image-guided treatment delivery, which enables better and more precise treatments for patients.

Based on the data set previously measured on the Linear accelerator (LINAC) and CT simulator, TPS calculates three-dimensional (3D) dose distribution in a patient. Unfortunately, many cases of incorrect data imports and usage of TPS were published, which also led to accidents with lethal outcomes^{1,2}.

Namely, 28% of accidents in RT are due to the wrong TPS dose calculations caused by: poor knowledge of TPS, incorrect data entered in TPS and lack of TPS calculation quality assurance (QA) – QA TPS³. International recommendations are that the delivered dose of radiation in the patient is no more than 5% different than prescribed, and the incidence of TPS calculation errors is less than 3–4% depending on the complexity of the RT treatment and anatomy. On the other hand, sub-dosage of the tumor of 5% affects the reduction of the treatment curability by around 20%, which points to the importance of the accuracy and precision of each procedure performed during the implementation of RT treatment⁴.

Therefore, the implementation of the QA-TPS procedure (such as the End-to-End test) for TPS in RT is crucial for reducing the number of accidents. There are several studies that have helped develop guidelines and protocols for LINAC-based QA TPS for 3D Conformal Radiotherapy (3DCRT)⁵⁻⁸ and Intensity Modulated Radiotherapy (IMRT)^{9,10} depending on the calculation algorithm used in TPS^{11,12}. Nowadays, in addition to 3DCRT and IMRT radiation techniques, volumetric modulated arc therapy (VMAT) is also used in routine practice.

It is clear that preparation and implementation of an End-to-End test is of great importance, which is used to con-

Postojala je značajna razlika između fotonskih energija relativnih grešaka (dobijene su veće vrednosti za 16 MV u odnosu na 6 MV). Utvrđena je statistički značajno manja relativna greška za kost kod AAA u odnosu na AcurosXB.

Ključne reči: algoritmi; modeli, teorijski; radioterapija; radioterapija, kompjutersko planiranje; toraks.

trol the overall precision of the entire RT chain. It is made up of a set of practical tests conducted on a heterogeneous phantom. In general, the End-to-End test consists of recording a calibration curve on a CT simulator and comparing it with a reference (entered into TPS), as well as creating characteristic RT plans of all RT techniques, energies of photon beams and calculating algorithms, irradiation-prepared plans on LINAC and measuring doses in defined phantom positions (tissue types).

Based on the End-to-End test, we have launched a dosimetric study to investigate: a) whether there is a significant difference in the dosimetric calculation of TPS (for: 3DCRT, IMRT and VMAT radiation techniques) in relation to the value obtained by LINAC measuring in the phantom, b) whether there is a significant difference in the accuracy of the dosimetric calculation between the calculation algorithms Analytical Anisotropic Algorithm (AAA) and Acuros XB, depending on the type of tissue in which the dose is applied and on photon beam energies.

Methods

Under the same, standardized, methodological principles, this study investigated the influence of various RT factors: radiation techniques, photon beam energy, calculation algorithm and tissue types, in regards to the TPS calculated dose.

Dosimetric tests cover all techniques of external beam radiotherapy (EBRT) and anatomical structures are similar to those encountered while working with patients.

All-round testing was carried out at the same facility in a relatively short period of time by engaging the same professional team, which generally implies repeatability and accuracy of the measurement.

Phantom

In all segments of this study, the heterogeneous phantom CIRS Thorax002LFC (Computerized Imaging Reference Systems Inc., Norfolk, Virginia) was used. The phantom anatomically represents the average human torso (30 cm long, 30 cm wide and 20 cm thick). It is made of plastic water, lungs (density 0.21 g/cm³) and bone-spinal cord (1.6 g/cm³), with 10 cylindrical inserts where the ionization chamber can be placed (Figure 1) and the dose measured at the particular place. The phantom also has a set of inserts (muscle, bone, lung and adipose equivalent tissue) of the known relative electron densities (RED)¹³.

Scanning the phantom on a CT simulator

The Thorax002LFC phantom was scanned on a sixteen-slice CT simulator LightSpeed (GE, Boston, Massachusetts). The gantry width bore 80 cm diameter, at a voltage in the X ray tube of 120 kV (thorax protocol). First, it was scanned with inserts of the known electron density in order to obtain the CT calibration curve that is the ratio between RED and Hounsfield units (HU). The materials used are in the range of -1000 for air, 0 for water and 1,000 HU for materials that simulate the bone. The obtained curve was compared with the “reference” curve in TPS, which was created by scanning the CIRS 062M phantom (25 cm long, 33 cm wide and 27 cm dense) that possesses 16 inserts with a known RED under the same conditions of the CT simulator. Acceptable difference RED for the same HU value, between curves, was ± 0.02 (ie. ± 20 HU for the same RED value, except for water ± 5 HU)⁴. The second time, the Thorax002LFC phantom was scanned (thorax protocol) with the cor-

responding cylindrical tissue inserts (Figure 1), for the making of a set of RT plans in the TPS.

The creation of clinical RT plans for dosimetric measurements

For study purposes, in the EBRT radiotherapy planning system Varian Eclipse 13.6 (Varian, Medical Systems, Palo Alto, California), six RT plans were made, four 3DCRT⁵, one IMRT and VMAT¹⁰. All plans were made for two photon energies 6 MV and 16 MV, as well as for two calculating algorithms: AAA and Acuros XB. This way, the isodose distribution in the phantom was obtained, ie. we got the absolute dose in different tissues (measuring points).

The beams geometry and the isodose distribution, as well as the position of the measuring points of the 3DCRT plans, are shown in Figure 2, while the detailed parameters of the plans are given in Table 1.

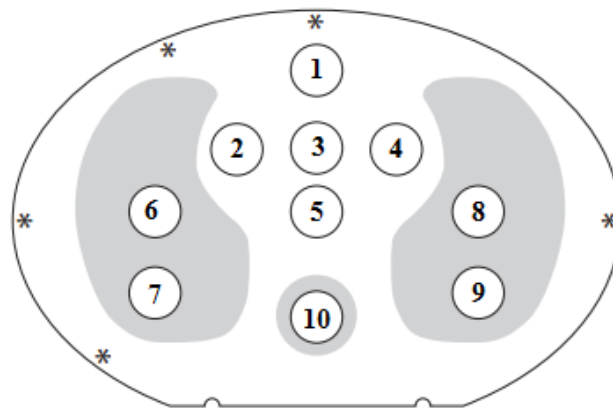


Fig. 1 – CIRS Thorax002LFC phantom with inserts for the soft tissue (1–5), lungs (6–9) and bone¹⁰.

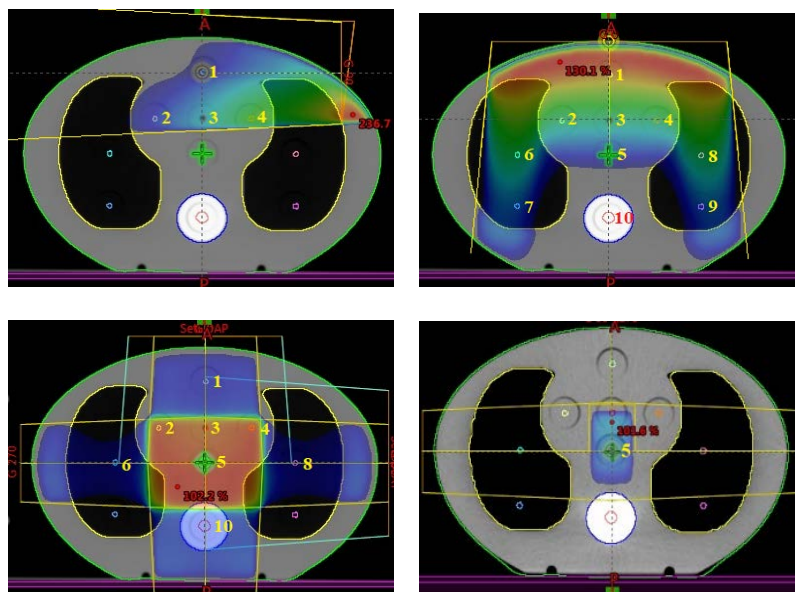


Fig. 2 – CIRS Thorax002LFC phantom with measuring points (1–10), beam geometry and isodose distribution for four 3DCRT RT plans (clinical tests 1–4).

For the purposes of making IMRT and VMAT RT plans, at the transverse CT slices of the CIRS Thorax002LFC phantom, planning target volume (PTV) and the heart are contoured at the length of 8 cm, while the lung and spinal cord are contoured to the entire length of the phantom (Figure 3)¹⁰. Detailed geometric-dosimetric parameters of these plans with dose limits for organs at risk (OAR) are given in Table 2.

Measurements on LINACs

The measurements were carried out on three Varian DHX LINACs (Varian Medical Systems, Palo Alto, California), with multi leaf collimator (MLC) Millennium120 and

nominal photon energies of 6 MV and 16 MV. One of the LINACs has no option of VMAT delivering.

To measure the absolute dose in the defined measuring positions of the Thorax002LFC phantom, we used the PTW-Semiflex 0.125 cm³ ionization chamber (Freiburg, Germany) with the SuperMax electrometer (Standard Imaging Inc., Middleton, Wisconsin). The ionization chamber and the electrometer were previously calibrated in the secondary standard dosimetry laboratory. Measurement uncertainty (for the measuring chain) is expressed as combined and expanded measurement uncertainty with expansion factor $k = 2$ (95%).

The absorbed dose at all the measuring points was determined based on the IAEA TRS 398 protocol¹⁴. In the lungs and materials equivalent to the bone, doses are meas-

Table 1

Geometric parameters of 3DCRT plans

Clinical test 1	Clinical test 2	Clinical test 3	Clinical test 4
SSD 100 cm	SAD, isocentre at point 1	SAD, isocentre at point 5	SAD, isocentre at point 5
1 direct field	1 tangential field	4 fields-box	3 non-coplanar fields
FS 20 × 10 cm ²	FS 15 × 10 cm ²	FS AP and PA 15 × 10 cm ²	FS 4 × 4 cm ² , G 30°, C 0°, Table 90°
G and C angle 0°	G and C 90°, wedge 60°	FS LatLeft and Right 15 × 8 cm ²	FS LatLeft 4 × 16 cm ² , G 90°, C 60° LatRight 4 × 16 cm ² , G 270°, C 300°
Deliver 2 Gy to point 3	Deliver 2 Gy to point 1	Deliver 2 Gy to point 5	Deliver 2 Gy to point 5
Measurement points: 1–10	Measurement points: 1–4	Measurement points: 1–6, 8, 10	Measurement point: 5

FS - field size; G - gantry; C - collimator.

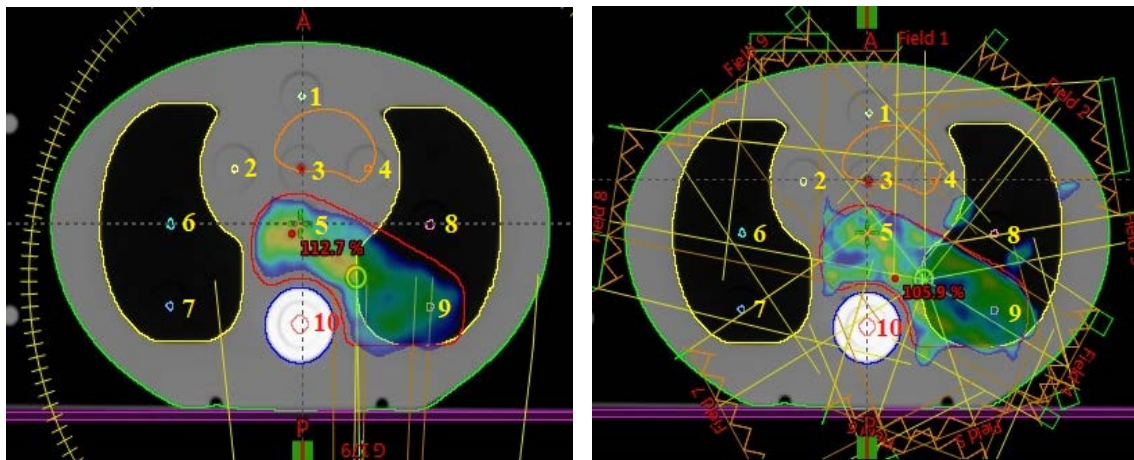


Fig. 3 – Intensity Modulated Radiotherapy (IMRT) and volumetric modulated arc therapy radiotherapy (VMAT RT) plans with beam geometry and isodose distributions, as well as the locations of measuring points (1–10).

Table 2

Geometric parameters of Intensity Modulated Radiotherapy (IMRT) and volumetric modulated arc therapy radiotherapy (VMAT RT) plans with dose limits for organ at risk (OAR)

Clinical test 5 IMRT	Clinical test 6 VMAT RT
SAD-9 IMRT fields	SAD-1 full arc
K 0°, G: 0, 40, 80, 120, 160, 200, 240, 260 and 320°	K 30°, G: 181–179°, clockwise
	Deliver 2 Gy to PTV (100% at target mean)
	Dose constraints for OAR
	Spinal cord: $D_{max} < 75\%$ of the prescribed dose
	Total lung: $D_{20\%} < 35\%$
	Heart: $D_{max} < 55\%$ of the prescribed dose
	Measurement points: 1–10

ured in small water volumes (the volume of ionization chamber) within these materials. Therefore, the measured doses in these points may have a larger error than the spots in plastic water. The influence of these small water volumes can be increasing the calculated dose up to 2% for a material equivalent to the lungs and 0.3% for a material equivalent to the bone¹⁵.

The total number of measuring points on three LINACs was 476, that is, 132 on LINAC 1 (92 for 3DCRT and 40 IMRT), 172 on LINAC 2 (92 3DCRT and 40 IMRT/VMAT) and 172 on LINAC 3 (92 3DCRT and 40 IMRT/VMAT). Divided by tissues, 280 measurements were done on soft tissue, 152 in the lungs, and 44 in the bone. Two hundred and thirty-eight measurements were done on photon beams 6 MV and 16 MV, as well as with calculating algorithms AAA and Acuros XB.

Statistical analysis

Due to a limited number of measuring positions in the Thorax002LFC phantom, the evaluation of the absolute dose values measured at each measuring position on LINAC (D_{meas}) and calculated on TPS (D_{cal}) was normalized with the dose measured at the reference point ($D_{\text{meas,ref}}$) for each test. Therefore, the equation for calculating the relative error is:

$$X (\%) = 100 * [(D_{\text{cal}} - D_{\text{meas}}) / D_{\text{meas,ref}}] \quad (1)$$

Allowed deviations for 3DCRT plans were 2–4%, while for IMRT/VMAT they were 3–4%.

Data are presented as arithmetic mean value with standard deviation (SD) or confidence interval (CI). The Kolmogorov-Smirnov test was applied to assess the normality of the studied continuous data.

Strength of the association between independent factors (accelerators, algorithms, tissues, photon energies, tests) and relative error data (dependent factor) were determined by using univariate and multiple linear regression analyses. Further detailed assessment was carried out using GLM univariate ANOVA (*post hoc* Bonferroni test) and Mann-Whitney U tests. All the analyses were estimated at minimal $p < 0.05$ level of statistical significance.

Complete statistical analysis of the data was done with the statistical software package SPSS Statistics 18 (USA).

Results

By measuring HU values for known RED values, we obtained the CT conversion curve for the CIRS Thorax002LFC phantom. The obtained curve was compared with the “reference” (TPS) curve, where the difference in the area of large electronic densities is seen, while in the lower density region, the match is within the allowed values. The RED values for bones (829 HU) differ by 3% while the difference in HU (RED 1.51) is 10% (Figure 4).

The differences between measured and TPS calculated doses at different measuring points (tissues) and RT plans (case 1–6), with values of tolerances (agreement criteria)

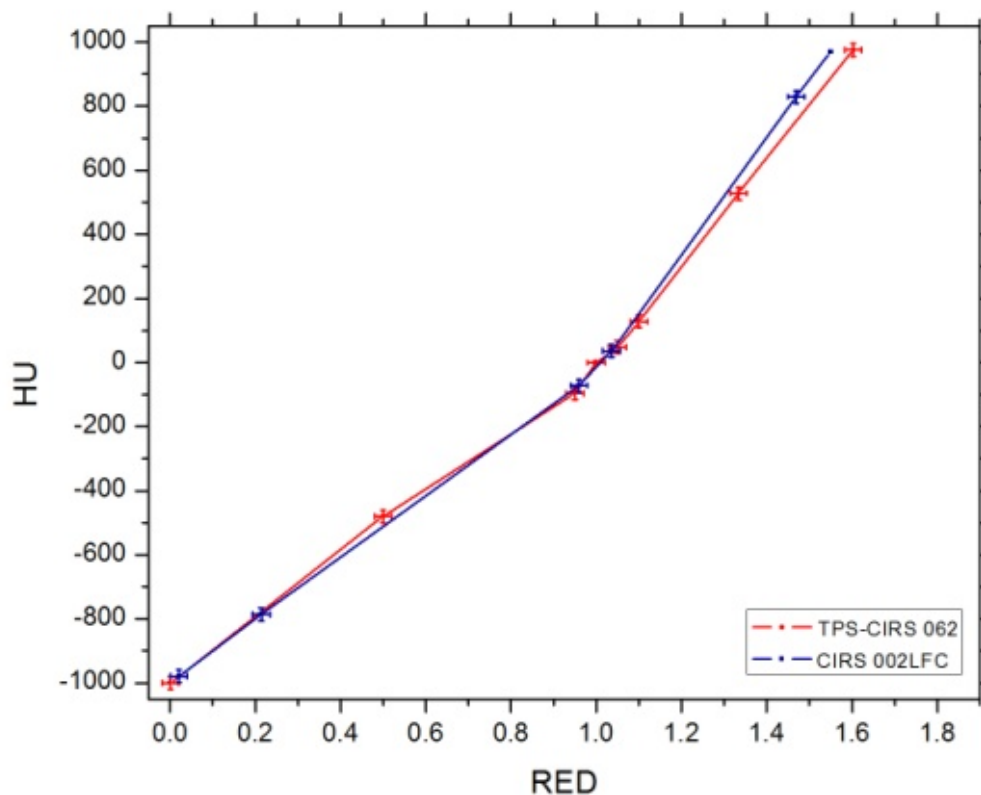


Fig. 4 – Shows of CT calibration curves obtained by CIRS Thorax002LFC and CIRS 062M phantom (“reference” curve located in treatment planning system –TPS).

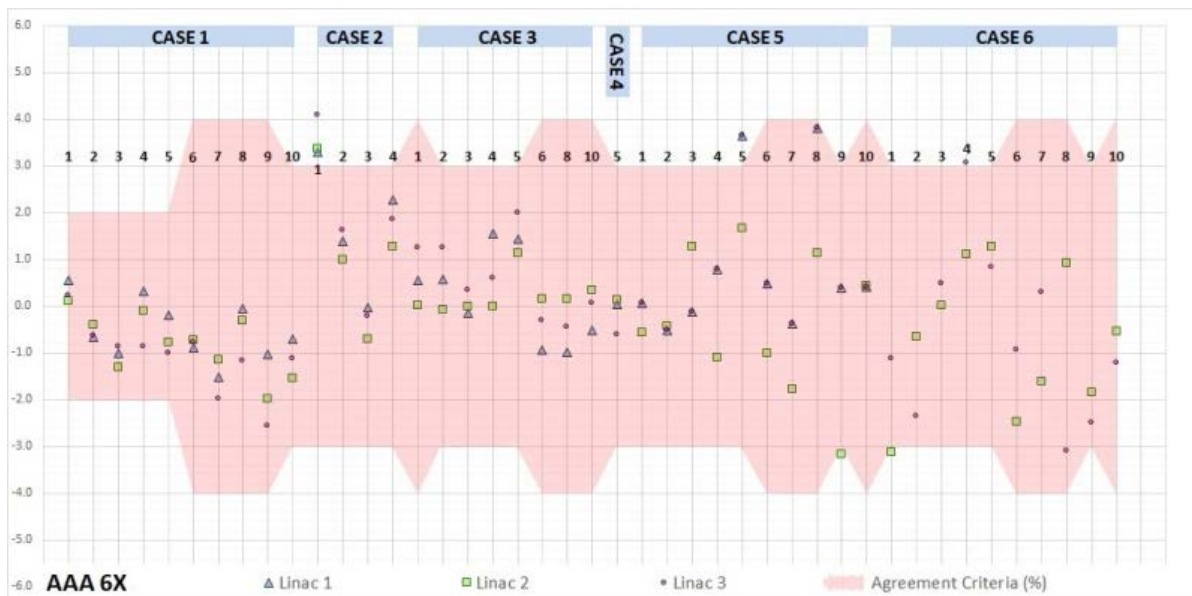
measured on three LINACs are presented in Figures 5 and 6. The results are grouped by calculating algorithms and photon beam energies.

Of the total 476 measuring points, the difference between measured and those TPS calculated doses greater than 4%, we had at 11 points (2.3%), 4–5% at 10 points (2.1%) and 5–6% at one position (0.2%). A 3–4% deviation was recorded at 19 measuring points (4%). The calculated (TPS) dose was in 353 cases (74.2%) lower than the measured and in 123 measurements (25.8%) higher.

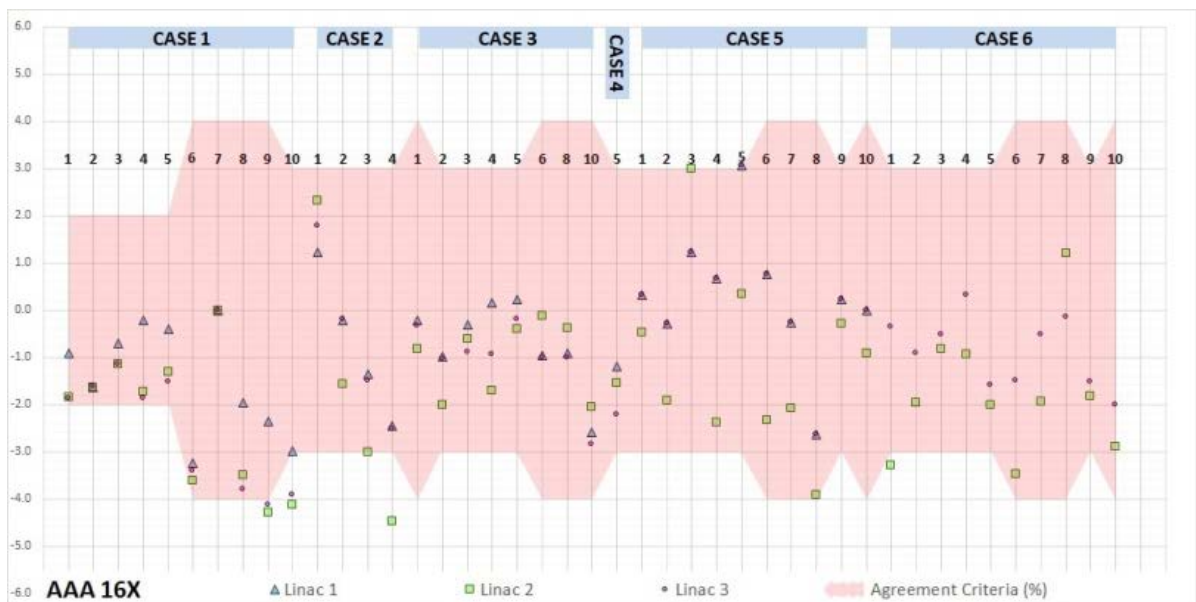
As Kolmogorov-Smirnov test revealed non-normal distribution of relative errors, some data transformation was necessary.

Firstly, negative sign marks obtained at any point, were corrected by adding corresponding fix value to all data. In this way, all relative errors have become positive. In the second part, these data were further transformed by applying $\log_{10}(X)$ transformation and used in all presented analyses.

Using the univariate and multivariate regression analyses, the effect of independent (explanatory) variables

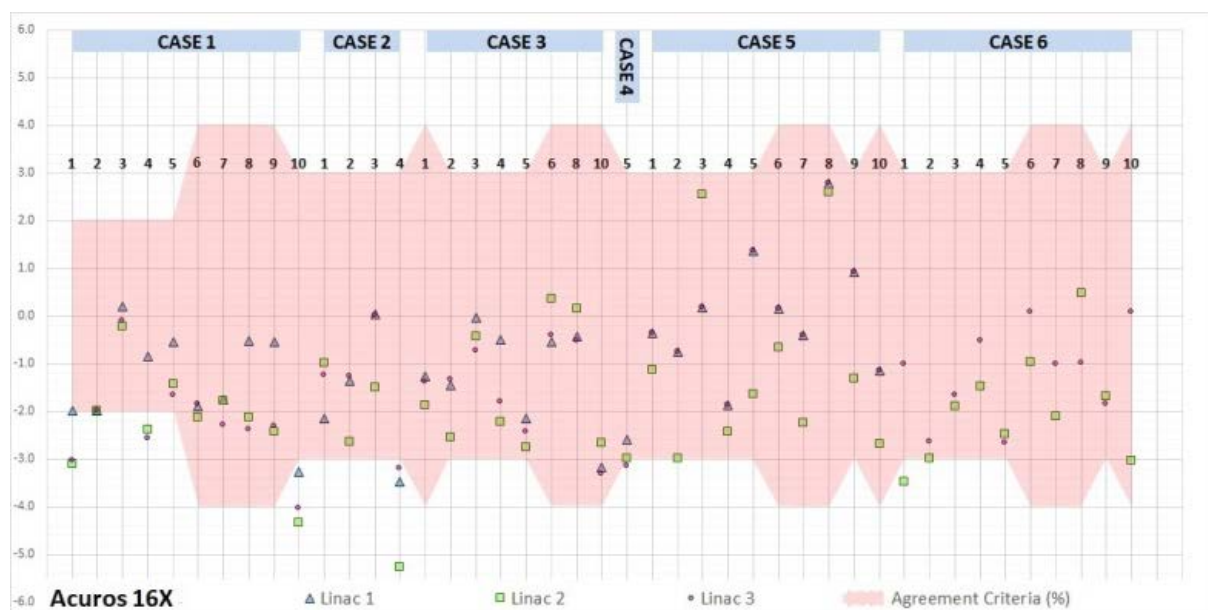


a)

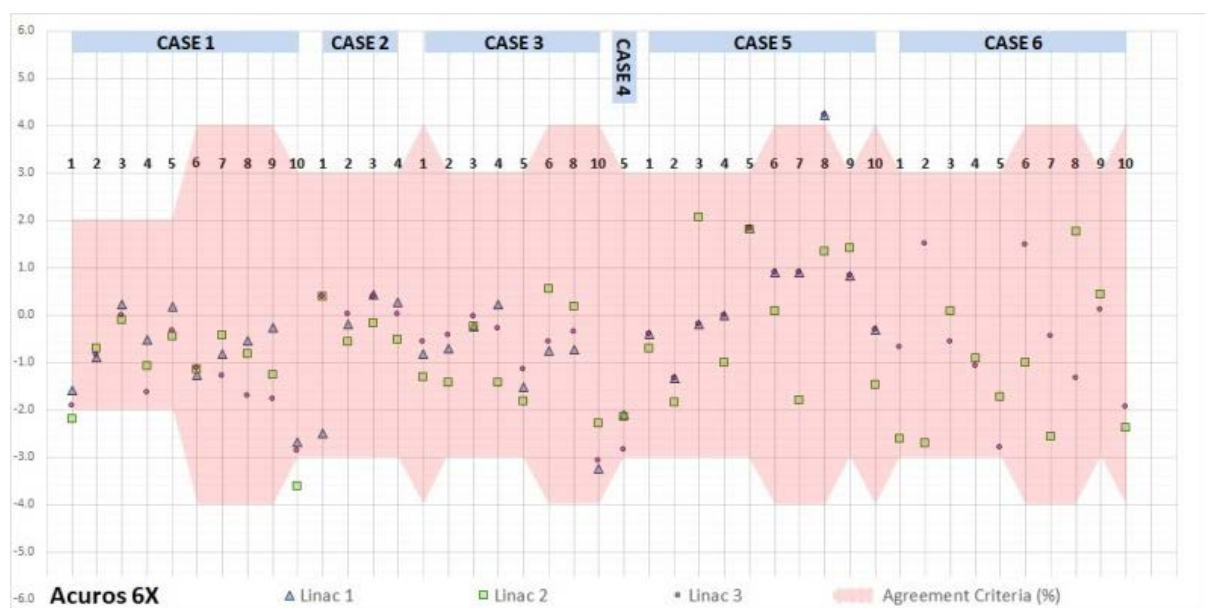


b)

**Fig. 5 – Difference between measured and treatment planning systems (TPS) calculated doses in each of the tests (cases) and measuring points for the Analytical Anisotropic Algorithm (AAA) calculation algorithm:
a) 6 MV photon beam; b) 16 MV photon beam.**



a)



b)

**Fig. 6 – Difference between measured and treatment planning systems (TPS) calculated doses in each of the tests (cases) and measuring points for the AcurosXB calculation algorithm:
a) 6 MV photon beam; b) 16 MV photon beam.**

on the relative errors X (%) was examined (Table 3).

Employing the univariate analysis of variance (GLM model, ANOVA), we examined the main effects of independent predictors on the relative error X (%), as it is presented in Table 4. Because of the large number of potential interactions of independent variables (total of 26), their effects on the measured results have not been shown.

For independent predictors, in which a statistically significant effect was found for the relative errors (devia-

tions), the significance of the differences between the mean values of the relative errors of certain categories was investigated, using the Bonferroni test (ie. steam comparisons). The overview of this analysis is given in Table 5.

In addition, we investigated the magnitude of the mean value of the relative errors, depending on the calculation algorithms and tissue types with the Mann-Whitney U test (Table 6).

Table 3**Univariate and multiple linear regression analysis of independent factors potentially associated with inaccurate dose calculation (measured vs. calculated).**

Independent variables	Univariate		Multiple	
	Beta (95% CI)	<i>p</i>	Beta (95% CI)	<i>p</i>
LINAC (1–3)	-0.013 (-0.018–0.013)	0.769	0.009 (-0.012–0.015)	0.825
Algorithm (AAA vs. Acuros XB)	0.112 (-0.006–0.054)	0.015	0.112 (0.009–0.052)	0.006
Tissue (soft vs. lung vs. bone)	0.259 (0.035–0.071)	< 0.001	0.272 (0.039–0.072)	< 0.001
Energy (6 MV vs 16 MV)	0.337 (-0.068–0.114)	< 0.001	0.337 (0.069–0.113)	< 0.001
Case (1–6)	-0.163 (0.005–0.018)	< 0.001	-0.183 (-0.007–0.019)	< 0.001

Beta – standardised regression coefficient; CI – confidence interval (unstandardized coefficient B).

Table 4**GLM univariate ANOVA (main effects of independent variables)**

Parameters	F	<i>p</i>
LINAC (1–3)	1.546	0.215
Algorithm (AAA vs. Acuros XB)	15.591	< 0.001
Tissue (soft tissue vs. lung vs. bone)	30.309	< 0.001
Energy (6 MV vs. 16 MV)	51.432	< 0.001
Case (1–6)	14.230	< 0.001

GLM – General Linear Model; AAA – Analytical Anisotropic Algorithm.

Table 5**Significance of differences in: calculating algorithms, tissue type, photon beam energy and radiation techniques (cases), using the Bonferroni test**

Parameters	Deviation (%), absolute values		<i>p</i> *
	n	mean ± SD	
Algorithm			
AAA (1)	238	1.36 ± 1.10	< 0.001 (1 : 2)
Acuros XB (2)	238	1.46 ± 1.06	
Tissue			
soft tissue (1)	280	1.26 ± 0.99	1.000 (1 : 2)
lung (2)	152	1.48 ± 1.10	< 0.001 (1 : 3)
bone (3)	44	2.10 ± 1.27	< 0.001 (2 : 3)
Photon beam energy			
6 MV (1)	238	1.12 ± 0.94	< 0.001 (1 : 2)
16 MV (2)	238	1.69 ± 1.13	
Case			
1	120	1.59 ± 1.15	< 0.001 (1 : 2)
2	48	1.51 ± 1.31	< 0.001 (1 : 3)
3	96	1.00 ± 0.87	< 0.001 (1 : 5)
4	12	1.80 ± 1.09	0.003 (1 : 6)
5	120	1.41 ± 1.07	0.033 (4 : 5)
6	80	1.50 ± 0.95	> 0.044 (5 : 6)

AAA – Analytical Anisotropic Algorithm; SD – standard deviation;

**post hoc* Bonferroni test.

Table 6**Algorithms and tissue depending differences**

Tissue	AAA		Acuros XB		<i>p</i> *
	Mean (%)	95% CI	Mean (%)	95% CI	
Soft	1.15	0.99–1.31	1.37	1.20–1.54	0.072
Lung	1.68	1.40–1.97	1.27	1.07–1.47	0.085
Bone	1.56	1.01–2.10	2.64	2.16–3.13	0.004

AAA – Analytical Anisotropic Algorithm; CI – confidence interval.

*Mann-Whitney *U* test.

Discussion

Based on the comparison of the reference and measured conversion curves, we established a difference in the area of higher electronic densities (RED values for bones vary by 3%), while in lower density areas, the match is within the allowed values (Figure 4). However, it is estimated that the difference of 8 in the bone relative electron density affects dose TPS calculation accuracy less than 1%¹⁶.

Out of the total 476 measuring points, the deviation between TPS calculated and measured doses of 3–6% was obtained in 30 measuring points (6.3%) (Figures 5 and 6).

The measured dose was in 188 (79%) cases higher than TPS calculated for Acuros XB, while in the case of AAA the same was noticed in 165 (69.3%) cases.

Depending on the tissue type, the measured dose in bone was in 88.6% of the cases higher than the calculated one, for the lungs in 76.3% and soft tissue in 70.7% of the cases.

When the bone tissue is analyzed independently, the Acuros XB led in 95.5% of points to the increased measured dose in relation to the calculated (81.8% in the case of the AAA algorithm application).

Based on the univariate and multivariate regression analyses, we could notice a significant influence of calculating algorithms, tissue type, photon beam energy and test type (Cases 1–6) on the relative error (deviation) in both models (Table 3). These data indicate that these variables are significant independent predictors with an influence on the size of the relative error. Depending on the LINACs, there was no significant effect on the size of the relative error. Based on the value of the standardized Beta coefficient (Table 3), the greatest influence on the relative error was the photon beam energy (Beta = 0.337; 33.7%), then the tissue type (Beta = 0.272; 27.2), test types (Beta = -0.183; 18.3%) and the applied calculation algorithm (Beta = 0.112; 11.2%). The direction of the sign (+ or -) indicates that greater relative errors can be expected when using 16 MV in comparison to 6 MV (which is in accordance with the results of the studies by Rutonjski et al.¹⁵, Gershkevitch et al.¹⁷ and Knoos et al.¹⁸) in the bone tissue compared to the soft tissue and lungs, in tests cases 1 and 2 (compared to other cases) and in the application of the calculation algorithm Acuros XB vs. AAA.

Using the univariate analysis of variance (GLM model, ANOVA), this study confirmed significant effects on the relative error (previously obtained by univariate and multivariate regression analysis), depending on the applied calculation algorithm, type of tissue, photon beam energy and test type (Table 4).

If we focus on the specific research objectives of this study, the supplementary (*post hoc*) analysis (Bonferroni

test, Table 5) shows that the Acuros XB calculating algorithm leads to a statistically significant increase in the relative error compared to the AAA. The highest values of the relative error were registered for bone tissue (2.10 ± 1.27).

By comparing the AAA and Acuros XB calculating algorithms, a statistically significant difference in registered relative errors in the bone was shown (Table 6). The corresponding mean values and 95% of the confidence limit were 1.56% for the AAA algorithm and 2.64% for Acuros XB.

The fact that with the applied calculation algorithms there is no overlap of the 95% of confidence limits indicates a statistically significant difference for the bone. Applied calculating algorithms lead to approximately the same (statistically non-significant) relative errors in the soft tissue and lungs (which is opposite to the Schiefer et al.¹⁰ study, which established the same degree of accuracy of the two algorithms except for the lungs, where Acuros XB has a smaller relative error).

The design of the study also caused the appearance of certain weaknesses primarily in the statistical part of the examination. In the case of simultaneous examination of multiple independent variables (multiple regression analysis, GLM univariate ANOVA with multiple independent variables), ideally the highest reliability was obtained when the number of samples in each group was approximately the same. Phantom characteristics (the unequal number of measuring points related to the tissue type) significantly contributed to this problem.

The selected statistical methods due to their robustness and reliability, but also the fact that different statistical techniques confirm the results of the test, indicate that there is a large extent of correctness in our conclusions.

Conclusion

The performed End-to-End test on the heterogeneous phantom CIRS Thorax002LFC gives us a confirmation of the correct TPS dose calculation (for all EBRT techniques, photon beam energy, calculating algorithms and different tissue types) and delivery to a patient on LINAC in our RT center daily clinical practice. The mentioned phantom in practice can be used for control, but not for obtaining a reference calibration curve. The analysis of the results has showed that there is no statistically significant difference between the LINAC, but it exists between photon energies (greater relative errors can be expected when using 16 MV compared to 6 MV). In addition to the calculation algorithms (AAA vs Acuros XB), there were no significant differences in soft tissue and lung relative errors, but for the bone there was a difference in favor of AAA.

R E F E R E N C E S

1. International Atomic Energy Agency (IAEA). Lessons Learned from Accidental Exposures in Radiotherapy, Safety Reports Series No. 17. Vienna: IAEA; 2000.
2. IAEA. Investigation of an Accidental Exposure of Radiotherapy Patients in Panama. Vienna: IAEA. 2001.
3. Task Group on Accident Prevention and Safety in Radiation Therapy. Prevention of accidental exposures to patients undergoing radiation therapy. A report of the International Commission on Radiological Protection. Ann ICRP 2000; 30(3): 7–70.

4. Technical Reports Series No. 430. Commissioning and quality assurance of computerized planning systems for radiation treatment of cancer. Vienna: International Atomic Energy Agency; 2004.
5. IAEA-TECDOC-1583. Commissioning of radiotherapy treatment planning systems: testing for typical external beam treatment techniques. Report of the Coordinated Research Project (CRP) on Development of Procedures for Quality Assurance of Dosimetry Calculations in Radiotherapy. Vienna: International Atomic Energy Agency; 2008. (English, Russian)
6. *Mijnheer B, Olszewska A, Florin C, Hartmann G, Knows T, Rosendale JC*, et al. ESTRO Booklet No. 7. Quality assurance of treatment planning systems. Practical examples for non-IMRT photon beams. Brussels: ESTRO; 2005.
7. *Fraass B, Doppke K, Hunt M, Kutcher G, Starkschall G, Stern R*, et al. American Association of Physicists in Medicine Radiation Therapy Committee Task Group 53: quality assurance for clinical radiotherapy treatment planning. *Med Phys* 1998; 25(10): 1773–829.
8. AAPM. Report No. 055 – Radiation Treatment Planning Dosimetry Verification 1995. Alexandria, VA: AAPM American Association of Physicists in Medicine; 1995.
9. TG-119 IMRT Commissioning Tests Instructions for Planning, Measurement, and Analysis Version 10/21/2009. Alexandria, VA: AAPM American Association of Physicists in Medicine; 2009.
10. *Schiefer H, Fogliata A, Nicolai G, Cozzi L, Selenga W, Born E*, et al. The Swiss IMRT dosimetry intercomparison using a thorax phantom. *Med Phys* 2010; 37(8): 4424–31.
11. *Gifford K, Followill D, Liu H, Starkschall G*. Verification of the accuracy of a photon dose–calculation algorithm. *J Appl Clin Med Phys* 2002; 3(1): 26–45.
12. *Brittan K, Rather S, Newcomb C, Murray B, Robinson D, Field C*, et al. Experimental validation of the Eclipse AAA algorithm. *J Appl Clin Med Phys* 2007; 8(2): 76–92.
13. CIRS Tissue Simulation & Phantom Technology. IMRT Thorax phantom Model 002LFC, user guide. Available from: www.cirsinc.com/radiation-therapy
14. Technical Reports Series No. 398. Absorbed dose determination in external beam radiotherapy. An International Code of Practice for Dosimetry Based on Standards of Absorbed Dose to Water. Vienna: International Atomic Energy Agency; 2000.
15. *Rutonjski L, Petrolija B, Baikal M, Teodorović M, Čudić O, Gersbkevič E*, et al. Dosimetric verification of radiotherapy treatment planning systems in Serbia: national audit. *Radiat Oncol* 2012; 7(1): 155.
16. *Thomas SJ*. Relative electron density calibration of CT scanners for radiotherapy treatment planning. *Br J Radiol* 1999; 72(860): 781–6.
17. *Gersbkevič E, Schmidt R, Velež G, Miller D, Korf E, Yip F*, et al. Dosimetric verification of radiotherapy treatment planning systems: results of IAEA pilot study. *Radiother Oncol* 2008; 89(3): 338–46.
18. *Knöös T, Wieslander E, Cozzi L, Brink C, Fogliata A, Albers D*, et al. Comparison of dose calculation algorithms for treatment planning in external photon beam therapy for clinical situations. *Phys Med Biol* 2006; 51(22): 5785–807.

Received on April 11, 2020

Revised on April 18, 2020

Accepted on July 6, 2020

Online July, 2020